Bounded Energy States in Homogeneous Turbulent Shear Flow—An Alternative View

P. S. Bernard
Department of Mechanical Engineering,
University of Maryland,
College Park, MD 20742

C. G. Speziale
Institute for Computer Applications in
Science and Engineering,
NASA Langley Research Center,
Hampton, VA 23665

The equilibrium structure of homogeneous turbulent shear flow is investigated from a theoretical standpoint. Existing turbulence models, in apparent agreement with physical and numerical experiments, predict an unbounded exponential time growth of the turbulent kinetic energy and dissipation rate; only the anisotropy tensor and turbulent time scale reach a structural equilibrium. It is shown that if a residual vortex stretching term is maintained in the dissipation rate transport equation, then there can exist equilibrium solutions, with bounded energy states, where the turbulence production is balanced by its dissipation. Illustrative calculations are presented for a $k-\epsilon$ model modified to account for net vortex stretching. The calculations indicate an initial exponential time growth of the turbulent kinetic energy and dissipation rate for elapsed times that are as large as those considered in any of the previously conducted physical or numerical experiments on homogeneous shear flow. However, vortex stretching eventually takes over and forces a production-equals-dissipation equilibrium with bounded energy states. The plausibility of this result is further supported by independent calculations of isotropic turbulence which show that when this vortex stretching effect is accounted for, a much more complete physical description of isotropic decay is obtained. It is thus argued that the inclusion of vortex stretching as an identifiable process may have greater significance in turbulence modeling than has previously been thought and that the generally accepted structural equilibrium for homogeneous shear flow, with unbounded energy growth, could be in need of re-examination.

1 Introduction

Homogeneous turbulent shear flow has been the subject of a variety of experimental, computational, and theoretical studies during the past four decades. The popularity of this flow lies in the fact that it accounts for an important physical effect—the alteration of the turbulence structure by shear—in a simplified setting unencumbered by such complications as rigid boundaries and mean turbulent diffusion. Von Karman (1937) first proposed the problem of homogeneous shear flow which gave rise to some mathematical studies during the 1950's (c.f. Townsend, 1956 and Hinze, 1975 for a review). It is a difficult flow to simulate experimentally and the first tangible suggestion for its generation was put forth by Corrsin (1963). The first successful experimental realization of homogeneous shear flow in the laboratory was achieved by Rose (1966) and was then followed by a series of landmark experiments by Champagne et al. (1970), Harris et al. (1977) and Tavoularis and Corrsin (1981). More recently, Tavoularis and Karnik (1989) and Rohr et al. (1988) performed more exhaustive measurements of homogeneous shear flow shedding new light on its basic structure.

With the dramatic increase in computer capacity achieved by the late 1970's, direct numerical simulations of homogeneous turbulent flows became possible. Rogallo (1981) was the first to conduct a direct simulation of homogeneous shear flow; the results that he obtained were well within the range of the experiments of Tavoularis and Corrsin (1981). Subsequently, Bardina et al. (1983) performed a coarse-grid large-eddy simulation of homogeneous shear flow and Rogers et al. (1986) conducted fine-grid $128 \times 128 \times 128$ direct simulations which further clarified its structure.

The early experiments of Rose (1966) and Champagne et al. (1970), which were conducted for relatively weak shear rates and small elapsed times, seemed to indicate that the Reynolds stresses—and, hence, the turbulent kinetic energy—asymptoted to equilibrium values. This asymptotic state is consistent with the production-equals-dissipation equilibrium that had been hypothesized by Townsend (1956) several years earlier. However, the integral length scales were still growing monotonically at the end of the Rose (1966) and Champagne et al. (1970) experiments suggesting the strong possibility that, an asymptotic state had not yet been reached. Subsequent physical experiments (Tavoularis and Corrsin, 1981; Tavoularis and Karnik, 1989; and Rohr et al., 1988) and direct numerical simulations (Rogallo, 1981; Bardina et al., 1983; and Rogers et al., 1986), conducted for stronger shear rates and larger elapsed times, confirmed this. These physical and numerical

Contributed by the Fluids Engineering Division for publication in the JOURNAL OF FLUIDS ENGINEERING. Manuscript received by the Fluids Engineering Division May 6, 1991.

experiments, along with alternative theoretical analyses (see Rogallo, 1981 and Tavoularis, 1985), have led to the following widely accepted physical picture of homogeneous shear flow:

(1) the turbulent kinetic energy k and dissipation rate ϵ grow exponentially in time at the same rate,

(2) the anisotropy tensor b_{ij} and the dimensionless turbulent time scale Sk/ϵ reach equilibrium values that are relatively independent of the initial conditions and the shear rate S.

It should be noted that Speziale and MacGiolla Mhuiris (1989) have recently shown that virtually all of the commonly used two-equation turbulence models and second-order closures are consistent with this hypothetical picture of homogeneous shear flow.

An alternative physical picture of homogeneous shear flow is presented in this paper which is consistent with the previously conducted physical and numerical experiments, yet at the same time excludes the occurrence of unbounded energy growth. In particular, it will be shown that when the effect of vortex stretching is maintained in the dissipation rate transport equation, a production-equals-dissipation equilibrium results in which the turbulent kinetic energy and dissipation rate eventually asymptote to bounded values. Illustrative calculations are presented for a $k-\epsilon$ model suitably modified to account for vortex stretching. Consistent with physical and numerical experiments, these calculations indicate an exponential time growth of the turbulent kinetic energy and dissipation rate for $St < 30$. This is the largest elapsed time considered in any of these previous experimental studies. However, for $St > 30$, vortex stretching eventually takes over causing the system to saturate and attain an equilibrium structure with bounded kinetic energy and dissipation. In the sections to follow, a detailed case is made to establish that this alternative equilibrium structure of homogeneous shear flow is a serious possibility that could have important implications for turbulence modeling at high Reynolds numbers.

2 Theoretical Background

We will consider the incompressible and isothermal turbulent flow of a viscous fluid. The governing field equations are the Navier-Stokes and continuity equations given by

$$\frac{\partial v_i}{\partial t} + v_j \frac{\partial v_i}{\partial x_j} = -\frac{\partial P}{\partial x_i} + \nu \nabla^2 v_i \tag{1}$$

$$\frac{\partial v_i}{\partial x_i} = 0 \tag{2}$$

where v_i is the velocity vector, P is the modified pressure and ν is the kinematic viscosity of the fluid. As in the usual treatments of turbulence, the velocity and pressure will be decomposed into ensemble mean and fluctuating parts, respectively:

$$v_i = \overline{v}_i + u_i,\ P = \overline{P} + p. \tag{3}$$

For homogeneous shear flow, the mean velocity-gradient tensor takes the form

$$\frac{\partial \overline{v}_i}{\partial x_j} = \begin{pmatrix} 0 & S & 0 \\ 0 & 0 & 0 \\ 0 & 0 & 0 \end{pmatrix}. \tag{4}$$

In direct numerical simulations of homogeneous shear flow, an initially isotropic turbulence is subjected to the constant shear rate S and its time evolution is then computed. In laboratory experiments, an initially decaying isotropic turbulence, created downstream of a grid, is subjected to a uniform shear rate as it evolves spatially. The two problems are related, in an *approximate* sense, by the Galilean transformation

$$x = x_0 + U_c t \tag{5}$$

where U_c is a characteristic mean velocity that is typically taken to be the centerline mean velocity of the uniform shear [hence, dimensionless time $St \equiv S(x - x_0)/U_c$]. For the remainder of this paper, we will only consider the temporally evolving version of homogeneous shear flow, since it is the only version of this problem that is *exactly* homogeneous.

In any homogeneous turbulent flow, the exact transport equations for the turbulence kinetic energy $k \equiv \frac{1}{2}\overline{u_i u_i}$ and dissipation rate $\epsilon \equiv \nu \overline{\frac{\partial u_i}{\partial x_j}\frac{\partial u_i}{\partial x_j}}$ take the form (Tennekes and Lumley, 1972)

$$\dot{k} = \mathcal{P} - \epsilon \tag{6}$$

$$\dot{\epsilon} = \mathcal{P}_{\epsilon_S} + \mathcal{P}_{\epsilon_V} - \Phi_\epsilon \tag{7}$$

where

$$\mathcal{P} = -\tau_{ij}\frac{\partial \overline{v}_i}{\partial x_j},\ \mathcal{P}_{\epsilon_S} = 2\nu\, \overline{\omega_i \omega_j}\, \frac{\partial \overline{v}_i}{\partial x_j}, \tag{8}$$

$$\mathcal{P}_{\epsilon_V} = 2\, \overline{\omega_i \omega_j \frac{\partial u_i}{\partial x_j}},\ \Phi_\epsilon = 2\nu^2\, \overline{\frac{\partial \omega_i}{\partial x_j}\frac{\partial \omega_i}{\partial x_j}}, \tag{9}$$

are, respectively, the production of turbulent kinetic energy, the production of dissipation by mean strains, the production of dissipation by vortex stretching, and the destruction of dissipation. In (8)–(9), $\tau_{ij} \equiv \overline{u_i u_j}$ is the Reynolds stress tensor and $\omega \equiv \nabla \times \mathbf{u}$ is the fluctuating vorticity vector. At this stage, we introduce the anisotropy tensor b_{ij} defined as

$$b_{ij} = \frac{\left(\tau_{ij} - \frac{2}{3}k\delta_{ij}\right)}{2k} \tag{10}$$

which will be useful in the analysis to follow.

If we non-dimensionalize the turbulent kinetic energy, dissipation rate, and time as follows:

$$k^* \equiv \frac{k}{k_0},\ \epsilon^* \equiv \frac{\epsilon}{\epsilon_0},\ t^* \equiv St,$$

where k_0 and ϵ_0 denote initial values, then the exact transport Eq. (6) for k can be rewritten in the dimensionless form

$$\dot{k}^* = 2\left(\frac{\epsilon}{\mathcal{P}} - 1\right) b_{12} k^* \tag{11}$$

since $\mathcal{P} = -\tau_{12}S$ in homogeneous shear flow. It should be noted that the ratio of production to dissipation $\mathcal{P}/\epsilon$ can be related to b_{12} through the identity

$$\frac{\mathcal{P}}{\epsilon} = -2b_{12}\frac{Sk}{\epsilon}. \tag{12}$$

Consequently, if any two of the quantities $\mathcal{P}/\epsilon$, b_{12} and Sk/ϵ are known, the remaining one can be computed using (12). Furthermore, since for homogeneous shear flow $\mathcal{P}/\epsilon > 0$ and $Sk/\epsilon > 0$, it follows from (12) that $b_{12} < 0$. Physical and numerical experiments have tended to indicate that b_{12} and Sk/ϵ reach equilibrium values that are relatively independent of the initial conditions. More specifically, these experiments suggest the results

$$\left(\frac{Sk}{\epsilon}\right)_\infty \approx 6.0,\ (b_{12})_\infty \approx -0.15,\ \left(\frac{\mathcal{P}}{\epsilon}\right)_\infty \approx 1.8 \tag{13}$$

where $(\cdot)_\infty$ is the equilibrium value obtained in the limit as $t \to \infty$. From (11) and (13) it follows that for $t^* \gg 1$,

$$k^* \sim \exp(\lambda t^*) \tag{14}$$

where the growth rate λ is given by

$$\lambda = 2\left[\left(\frac{\epsilon}{\mathcal{P}}\right)_\infty - 1\right](b_{12})_\infty \approx 0.13. \tag{15}$$

Equations (13) and (14) then imply that for $t^* \gg 1$

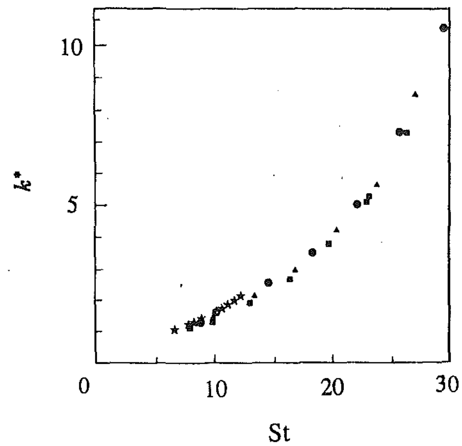

Fig. 1 Experimental data on homogeneous shear flow measured by Tavoularis and Corrsin (1981) and Tavoularis and Karnik (1989) (as compiled by Rohr et al. (1988)).

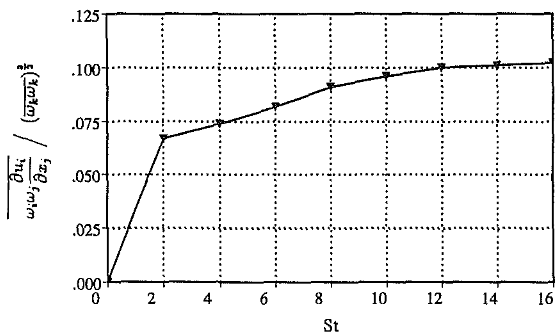

Fig. 2 Time evolution of the normalized vortex stretching in homogeneous shear flow obtained from the direct numerical simulation (case C128U) of Rogers (1990).

$$\epsilon^* \sim \exp(\lambda t^*) \tag{16}$$

since, if k grows exponentially and Sk/ϵ equilibrates, then ϵ must grow exponentially at the same rate. This constitutes an alternate derivation of the Tavoularis (1985) asymptotic law of exponential growth in shear flow. The wealth of experimental data on homogeneous shear flow collected over the past two decades appears to be in agreement with this hypothetical physical picture. This is evidenced by Fig. 1 containing several sets of measured k data versus nondimensional time that was recently compiled by Rohr et al. (1988).

The occurrence of this structural equilibrium at large times—with an unbounded exponential time growth of k and ϵ—has a number of implications for the higher-order correlations in the dissipation rate transport Eq. (7) which will now be examined. When non-dimensionalized, (7) takes the form

$$\dot{\epsilon}^* = \left(\frac{2\overline{\omega_1\omega_2}}{\overline{\omega_k\omega_k}} + \frac{2\overline{\omega_i\omega_j \frac{\partial u_i}{\partial x_j}}}{(\overline{\omega_k\omega_k})^{3/2}} \frac{\epsilon}{Sk}\sqrt{R_t} - \frac{2\nu}{S}\frac{\overline{\frac{\partial \omega_i}{\partial x_j}\frac{\partial \omega_i}{\partial x_j}}}{\overline{\omega_k\omega_k}} \right)\epsilon^* \tag{17}$$

where $R_t \equiv k^2/\nu\epsilon$ is the turbulence Reynolds number. In deriving (17), use has been made of the fact that $\epsilon \equiv \nu\overline{\omega_i\omega_i}$ since the turbulence is homogeneous. According to the Schwarz inequality, the first of the three correlations

$$\frac{\overline{\omega_1\omega_2}}{\overline{\omega_k\omega_k}}, \quad \frac{\overline{\omega_i\omega_j \frac{\partial u_i}{\partial x_j}}}{(\overline{\omega_k\omega_k})^{3/2}}, \quad \frac{2\nu\,\overline{\frac{\partial \omega_i}{\partial x_j}\frac{\partial \omega_i}{\partial x_j}}}{S\,\overline{\omega_k\omega_k}}$$

appearing in (17) will be bounded for all time. In addition, direct numerical simulations of Rogers (1990) for homogeneous shear flow, as shown in Fig. 2, indicate that the second of these correlations (which is proportional to the velocity derivative skewness S_K in an isotropic turbulence) asymptotes fairly quickly to an apparent equilibrium value of 0.1. Hence, assuming the equilibration of ϵ/Sk, it follows that in order to recover the exponential growth law (16) for $t^* \gg 1$, we must have the third of these correlations behave as

$$\frac{\nu}{S}\frac{\overline{\frac{\partial \omega_i}{\partial x_j}\frac{\partial \omega_i}{\partial x_j}}}{\overline{\omega_k\omega_k}} = C_\omega\sqrt{R_t} + O(1), \tag{18}$$

where the coefficient C_ω must assume the precise value

$$C_\omega = \left(\frac{\overline{\omega_i\omega_j \frac{\partial u_i}{\partial x_j}}}{(\overline{\omega_k\omega_k})^{3/2}} \right)_\infty \left(\frac{\epsilon}{Sk}\right)_\infty. \tag{19}$$

The general R_t dependence indicated by (18) is consistent with traditionally accepted Kolmogorov scaling laws for the case of homogeneous turbulence. However, the validity of (19) in homogeneous shear flow is debatable. Direct numerical simulations of homogeneous shear flow by Rogers (1990) are not conclusive concerning the validity of (18) or (19). Furthermore, it may be argued that it is unlikely that the effect of vortex stretching would be *exactly* counterbalanced by the leading order part of a viscous term in an unstable high Reynolds number turbulent flow with an exponentially growing turbulent kinetic energy; one might expect vortex stretching to play an independent role in such a shear instability. The ultimate equilibrium state that a homogeneous turbulent flow achieves is determined by how the fundamental imbalance between vortex stretching and the mean production and viscous destruction terms is resolved (this imbalance arises since only the vortex stretching term depends *explicitly* on R_t). Consequently, to externally impose a balance, such as that implied by (18) and (19)-rather than to allow the balance to arise naturally from the equations of motion - runs the risk of yielding spurious equilibrium states. For the case of isotropic turbulence discussed later, it will be shown that at high turbulence Reynolds numbers an imbalance between vortex stretching and viscous dissipation drives the flow toward a $k \sim t^{-1}$ power law decay. If vortex stretching is neglected, however, this physical feature is lost and the exponent of the power law decay becomes completely arbitrary.

An examination of (17) suggests that there are two alternative equilibrium states for homogeneous shear flow apart from (13)-(14). These are:

(1) an alternative structural equilibrium where $(\epsilon/Sk)_\infty = 0$, or

(2) a production-equals-dissipation equilibrium with bounded energy states (i.e., with $k_\infty < \infty$ and $\epsilon_\infty < \infty$).

The first of these cases has been shown by Speziale and MacGiolla Mhuiris (1989) to be primarily associated with solutions for k and ϵ that undergo an algebraic growth with time (i.e., for $St \gg 1$, $k \sim t^\alpha$, $\epsilon \sim t^\beta$ where $\alpha > \beta$). Such solutions, however, are largely unstable within the context of Reynolds stress transport models (Speziale and MacGiolla Mhuiris, 1989). Furthermore, at the end of all of the previously conducted physical and numerical experiments on homogeneous shear flow, ϵ/Sk either appeared to equilibrate to a non-zero value or continued to grow - results that are not suggestive of an equilibrium state where $(\epsilon/Sk)_\infty = 0$. Hence, we conclude that this alternative equilibrium structure is not a strong possibility.

The second possibility—namely, the production-equals-dissipation equilibrium— superficially appears to contradict the physical and numerical experiments indicating that the turbulent kinetic energy and dissipation rate are still growing exponentially at the end of the experiments (i.e., for elapsed times St as large as 28). However, a production-equals-dissipation equilibrium wherein

$$\mathcal{P}_\infty = \epsilon_\infty \tag{20}$$

$$\Phi_{\epsilon_\infty} = \mathcal{P}_{\epsilon_{S\infty}} + \mathcal{P}_{\epsilon_{V\infty}} \tag{21}$$

(with bounded values for k_∞, ϵ_∞, and $R_{t\infty}$) is not inconsistent with either the ensemble averaged or mean spectral form of the Navier-Stokes equations (Hinze, 1975). In the following sections, it will be shown that the inclusion of vortex stretching effects in the dissipation rate transport equation leads to the occurrence of this production-equals-dissipation equilibrium (with an early exponential time growth of k and ϵ for $St < 30$). Furthermore, when such effects are included in the description of isotropic turbulence, a more complete physical description results.

3 The Dissipation Rate Transport Equation With Vortex Stretching

Batchelor and Townsend (1947) have shown that the transient behavior of the enstrophy $\omega^2 \equiv \overline{\omega_i\omega_i}$ in isotropic turbulence is governed by the equation

$$\frac{d\omega^2}{dt} = \frac{7}{3\sqrt{15}}\,\omega^3\,S_K - \frac{14}{3\sqrt{15}}\,\omega^3\,\frac{G}{R_\lambda} \tag{22}$$

where

$$S_K = -\frac{\overline{\left(\frac{\partial u}{\partial x}\right)^3}}{\left[\overline{\left(\frac{\partial u}{\partial x}\right)^2}\right]^{\frac{3}{2}}} \tag{23}$$

is the skewness of the probability density function of $\frac{\partial u}{\partial x}$ defined with a negative sign to make it a positive quantity. In (22), $R_\lambda \equiv u_{\rm rms}\,\lambda/\nu$ is the turbulence Reynolds number based on the Taylor microscale and G is a function defined by

$$G \equiv \lambda^4 f_o^{iv}. \tag{24}$$

Here, $u_{\rm rms}$ is the root-mean-square of a velocity fluctuation component u, λ is the Taylor microscale derived from the two point longitudinal velocity correlation function $f(r)$, and f_o^{iv} is the fourth derivative of $f(r)$ evaluated at $r = 0$. The first term on the right-hand side of (22) accounts for the effect of vortex stretching and is positive definite while the second term is always negative and leads to the destruction of enstrophy.

Equation (22) may be converted into a transport equation for ϵ through use of the identity

$$\epsilon = \nu\omega^2, \tag{25}$$

which is valid for any homogeneous turbulence. Since the defining equation for the microscale may be conveniently written as

$$\omega^2 = \frac{10k}{\lambda^2}, \tag{26}$$

it follows that (22) can be converted to the equation

$$\dot{\epsilon} = \frac{7}{3\sqrt{15}}\,\frac{S_K}{\sqrt{\nu}}\,\epsilon^{3/2} - \frac{7}{15}\,G\,\frac{\epsilon^2}{k}. \tag{27}$$

Once values are obtained for S_K and G, (27) may be solved together with the kinetic energy equation

$$\dot{k} = -\epsilon \tag{28}$$

yielding a solution for isotropic decay.

Batchelor and Townsend (1947) showed that if G has the form

$$G = \frac{30}{7} + \frac{1}{2}\,R_\lambda S_K, \tag{29}$$

then the solution of (27)-(28) is compatible with their experimental data indicating a power law decay of the kinetic energy, with an exponent of approximately one, for the case of moderately large values of R_λ. More precisely, the substitution of (29) into (27) yields the equation

$$\dot{\epsilon} = -2\frac{\epsilon^2}{k}, \tag{30}$$

which, when combined with (28), gives rise to the exact solution

$$k = k_0\left(1 + \frac{\epsilon_0 t}{k_0}\right)^{-1}$$

for isotropic decay (i.e., a power law decay where $k \sim t^{-1}$). Apart from the specific value of the numerical coefficient on the right-hand side of (30), which is more commonly set to a value ranging from 1.83-1.92 to reflect more recent decay data (Comte-Bellot and Corrsin, 1971) suggesting that $k \sim t^{-1.1}$ or $k \sim t^{-1.2}$, the form of (30) has served as a cornerstone for the standard modeled ϵ transport equation that is widely used in turbulence models.

In view of the identity $R_\lambda = \sqrt{20/3}\,R_t^{1/2}$, it is easily established that (29) is formally equivalent to the relation (18) introduced earlier in the case of homogeneous shear flow. As before, the choice of G given by (29) forces the vortex stretching term in (27) to be exactly subsumed by the action of the destruction of enstrophy term. While this step, as has been noted above, guarantees compatibility with isotropic decay data, it is also tantamount to imposing an equilbrium state on the flow rather than letting the equations of motion dictate the nature of the equilibrium. In this regard, it may be noted than (29) effectively excludes from consideration a family of exact self-similar solutions for isotropic decay depending explicitly on the distinction between vortex stretching and dissipation (see Sedov, 1944 and Bernard, 1985).

Another example of the breakdown of Eq. (29) arises in the limit of zero viscosity where the destruction of enstrophy term vanishes while the vortex stretching term does not. In fact, the survival of the vortex stretching term in the limit of zero viscosity is crucial for the prediction of enstrophy blow-up—a widely accepted property of solutions of the Euler equation (see Lesieur, 1990). This can be seen by setting ν equal to zero in (22) which yields the equation

$$\frac{d\omega^2}{dt} = \frac{7}{3\sqrt{15}}\,\omega^3\,S_K^{(0)} \tag{31}$$

where $S_K^{(0)}$ is the zero-viscosity skewness. For constant $S_K^{(0)} > 0$, (31) predicts that the enstrophy blows up at the critical time.

$$t_c = \frac{6\sqrt{15}}{7\omega_0}\,\frac{1}{S_K^{(0)}}$$

where ω_0^2 is the initial enstrophy. Although the Eddy-Damped Quasi-Normal Markovian (EDQNM) model supports this result, a finite-time enstrophy blow-up has not been seen in direct numerical simulations of the Euler equation (see Lesieur, 1990 and Pumir and Siggia, 1990). This means that either $S_K^{(0)}$ is a very small constant or a monotonically decreasing function of time (in the former case the enstrophy would blow-up at $t_c \gg \omega_0^{-1}$ whereas in the latter case it would just grow monotonically without bound as $t \to \infty$). While this issue has not been fully resolved, one thing is clear: $S_K^{(0)}$ is *not* identically zero. If $S_K^{(0)} = 0$, then (31) yields the erroneous prediction

$$\omega^2 = \text{constant}$$

which is not supported by direct numerical simulations or theoretical analyses of the Euler equation (these indicate that the enstrophy grows dramatically due to vortex stretching). The standard modeled dissipation rate Eq. (30) reduces to

$$\frac{d\omega^2}{dt} = 0$$

in the limit of zero viscosity and, hence, incorrectly predicts (in agreement with the $S_K^{(0)} = 0$ case) that the enstrophy is conserved.

We will now present an alternative model for the destruction of enstrophy term which maintains the effect of vortex stretching. The consequence of this model for both isotropic decay and homogeneous shear flow will be considered in turn. Consistent with the classical Kolmogorov scaling laws embodied in (18), we will set

$$\tau_0 \frac{2\nu \overline{\frac{\partial \omega_i}{\partial x_j} \frac{\partial \omega_i}{\partial x_j}}}{\overline{\omega_k \omega_k}} = C_{\omega_1} \sqrt{R_t} + C_{\omega_2} \quad (32)$$

where $\tau_0 \equiv k/\epsilon$ is the turbulent time scale and C_{ω_1} and C_{ω_2} are dimensionless constants. Since,

$$\frac{2\nu \overline{\frac{\partial \omega_i}{\partial x_j} \frac{\partial \omega_i}{\partial x_j}}}{\overline{\omega_k \omega_k}} = \frac{7}{15} G \frac{\epsilon}{k} \quad (33)$$

it follows that (32) is equivalent to the Batchelor and Townsend result (29) if $C_{\omega_1} = 7\, S_K/3\sqrt{15}$ and $C_{\omega_2} = 2$. The choice of $C_{\omega_1} = 7\, S_K/3\sqrt{15}$ represents the external imposition of an equilibrium structure on the turbulence where there is no net vortex stretching. In contrast to this approach, we will allow for small departures from equilibrium for which

$$C_{\omega_1} = \frac{7}{3\sqrt{15}} S_K - \eta_1 \quad (34)$$

where η_1 is a small parameter. In addition, we will consider small departures from the $O(1)$ term in the Batchelor and Townsend (1947) Eq. (29) by taking

$$C_{\omega_2} = 2 - \eta_2 \quad (35)$$

where η_2 is also a small parameter. Equation (29) is recovered in the limit as η_1 and η_2 go to zero. A direct substitution of (32) - (35) into (27) yields the modeled transport equation

$$\dot{\epsilon} = \frac{7}{3\sqrt{15}} \frac{C_{\epsilon_3}}{\sqrt{\nu}} \epsilon^{3/2} - C_{\epsilon_2} \frac{\epsilon^2}{k} \quad (36)$$

where $C_{\epsilon_3} = 3\sqrt{15}\eta_1/7$ and $C_{\epsilon_2} = 2 - \eta_2$. The coefficient C_{ϵ_3} is related to the zero viscosity skewness by

$$\lim_{\nu \to 0} C_{\epsilon_3} = S_K^{(0)} \quad (37)$$

and therefore (36), unlike the Batchelor and Townsend formula (30), can accommodate the limit of zero viscosity. Equation (36) is of the same general mathematical form as the ϵ-transport equation for self-preserving isotropic turbulence (see Speziale and Bernard, 1991). Thus there is a direct relation between the vortex stretching models proposed herein and the theory of self-preservation.

It will now be demonstrated that (36) gives a much more complete picture of isotropic turbulence than does the more commonly used ϵ-transport equation obtained in the limit as $C_{\epsilon_3} \to 0$. We will consider a small imbalance in the vortex stretching of the order of 1 percent, i.e., we will set $C_{\epsilon_3} =$

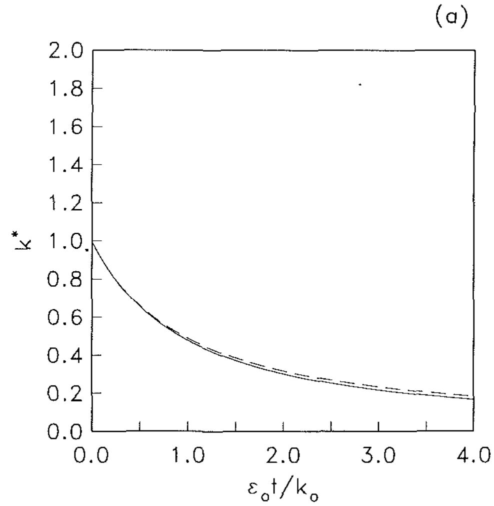

Fig. 3(*a*)

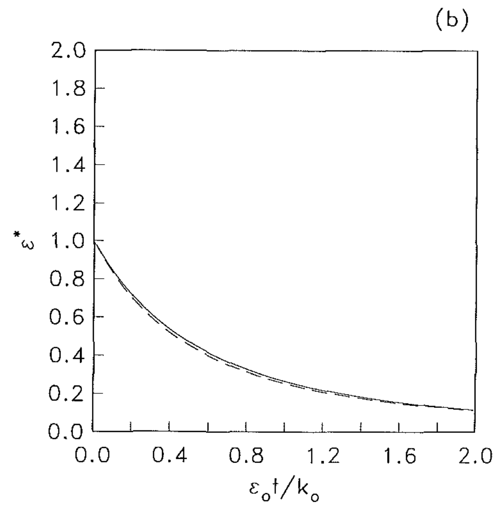

Fig. 3(*b*)

Fig. 3 Comparison of solutions for isotropic decay: ——— $k-\epsilon$ model with vortex stretching; --- standard $k-\epsilon$ model. (*a*) Time evolution of the turbulent kinetic energy for R_{t_o} = 300, and (*b*) time evolution of the turbulent dissipation rate for R_{t_o} = 300.

0.01. Consistent with the commonly used modeled ϵ-transport equation we set $C_{\epsilon_2} = 1.90$. For initial turbulence Reynolds numbers that are not extremely large, (36) has solutions that are almost identical to the standard model. This is illustrated in Figs. 3(*a*)-(*b*) showing the time evolution of the turbulent kinetic energy $k^* = k/k_0$ and turbulent dissipation rate $\epsilon^* = \epsilon/\epsilon_0$ for an initial turbulence Reynolds number $R_{t_0} = 300$. The differences between the new model and the standard model are negligible; both indicate a power law decay where $k \sim t^{-1.1}$.

The importance of including the vortex stretching term becomes evident in the case of extremely large values of R_{t_0} where there is a substantial difference between the two models. In Figs. 4(*a*)-(*b*) the early time evolution of the turbulent kinetic energy and dissipation rate are shown for an initial turbulence Reynolds number $R_{t_0} = 10^6$. Unlike the standard model, the new model (36) with vortex stretching predicts a dramatic rise in the dissipation rate (and hence the enstrophy) and a precipitous drop in the turbulent kinetic energy that is highly reminiscent of the prelude to enstrophy blow-up predicted by the EDQNM model. This point is made particularly clear by Fig. 4(*c*) showing the time evolution of the enstrophy for a range of increasing values of R_{t_0}. This result bears a strong resemblance to Fig. VI-4 given by Lesieur (1990).

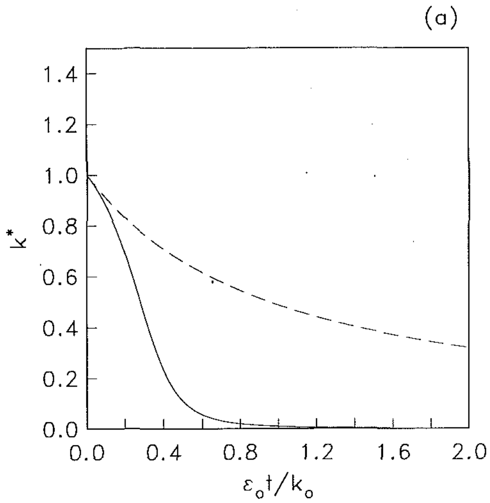

Fig. 4(*a*)

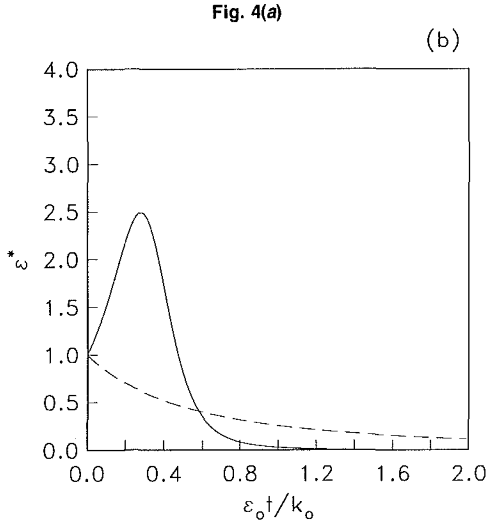

Fig. 4(*b*)

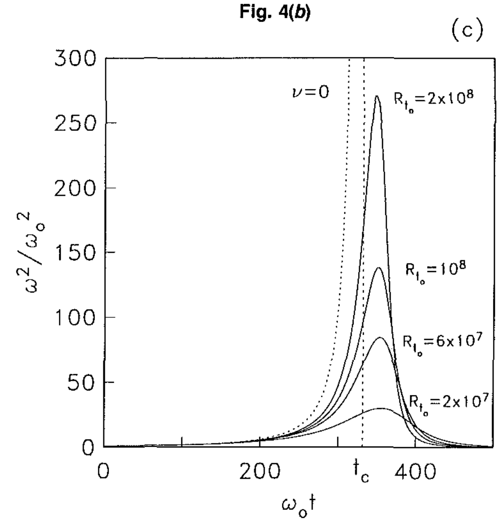

Fig. 4(*c*)

Fig. 4 Comparison of solutions for isotropic decay: ——— $k-\epsilon$ model with vortex stretching; --- standard $k-\epsilon$ model. (*a*) Time evolution of the turbulent kinetic energy for R_{t_o} = 10^6, (*b*) time evolution of the turbulent dissipation rate for R_{t_o} = 10^6, and (*c*) time evolution of the enstrophy for a variety of R_{t_o}.

The long time behavior of the solution for $R_{t_0} = 10^6$ is shown in Fig. 5. It is seen that after sufficiently large elapsed times (approximately 5–10 eddy turnover times), the turbulence be-

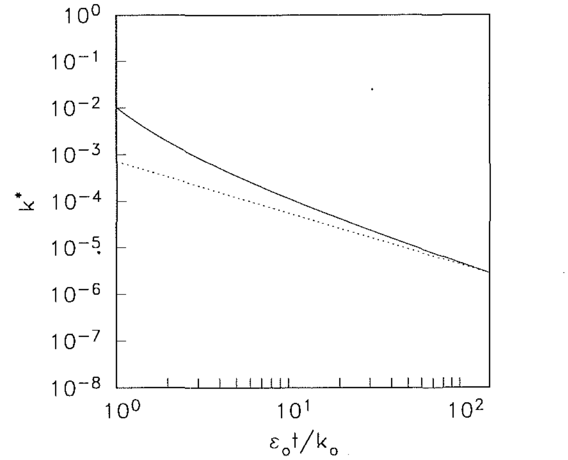

Fig. 5 Long time evolution of the turbulent kinetic energy in isotropic turbulence for R_{t_o} = 10^6. ——— $k-\epsilon$ model with vortex stretching (C_{ϵ_2} = 1.90, C_{ϵ_3} = 0.01); --- $k \sim t^{-1.1}$.

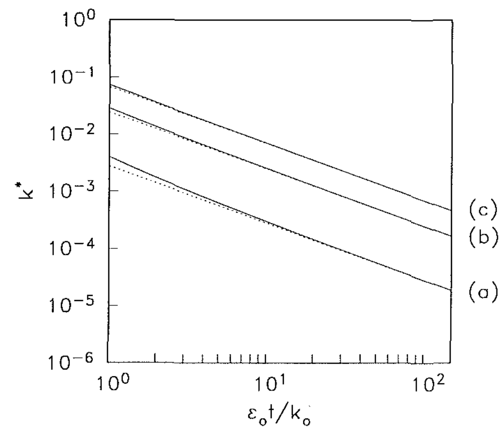

Fig. 6 Long time evolution of the turbulent kinetic energy in isotropic turbulence predicted by the $k-\epsilon$ model with vortex stretching for R_{t_0} = 10^7. (*a*) C_{ϵ_2} = 3, (*b*) C_{ϵ_2} = 5, and (*c*) C_{ϵ_2} = 7. (——— model; --- $k \sim t^{-1}$).

gins to approach a power law decay where $k \sim t^{-1.1}$. The duration of the early time transient, for a given initial turbulence Reynolds number $R_{t_0} \gg 1$, can be shown to become smaller with increasing values of C_{ϵ_2}. For $C_{\epsilon_2} > 2$, it is a simple matter to show that equation (36) has the simple fixed point

$$R_{t_\infty} = \left(\frac{C_{\epsilon_2} - 2}{\dfrac{7}{3\sqrt{15}}\, C_{\epsilon_3}} \right)^2. \tag{38}$$

This solution can be shown to correspond to a t^{-1} power law decay for the turbulent kinetic energy. Calculations are shown in Fig. 6 pertaining to three different values of $C_{\epsilon_2} > 2$ (C_{ϵ_2} = 3, 5 and 7) for an initial turbulence Reynolds number R_{t_0} = 10^7. It is clear that after an initial transient, the flow rapidly approaches an asymptotic solution where $k \sim t^{-1}$. This means that, in fact, the equilibrium exponent of the decay law can never be less than one, since for $C_{\epsilon_2} < 2$, the asymptotic solution is of the form $k \sim t^{-1/(C_{\epsilon_2}-1)}$. Furthermore, these results establish that for an isotropic turbulence to be close to equilibrium when R_{t_0} is extremely large, we must have $C_{\epsilon_2} >$ 2, otherwise the initial transient will be of a duration longer than an eddy turnover time (i.e., the flow will be significantly far from equilibrium).

For small R_t it is well known that the turbulent kinetic energy undergoes a power law decay with an exponent substantially greater than 1 – a condition that can be achieved by choosing $C_{\epsilon_2} < 2$. The implication is that C_{ϵ_2} is, in general, a function of the turbulence Reynolds number – a fact which has long been known to be the case. In summary, it may be stated that the ϵ-transport Eq. (36) with vortex stretching predicts the following physical picture of isotropic turbulence (see Speziale and Bernard, 1991):

(*a*) A power law decay where $k \sim t^{-\beta}$ (with $\beta \equiv 1/(C_{\epsilon_2} - 1) > 1$) for intermediate to low turbulence Reynolds numbers,

(*b*) for extremely high turbulence Reynolds numbers, an initial transient where there is a tendency toward enstrophy blow-up followed by a $k \sim t^{-1}$ power law decay, and

(*c*) a finite-time enstrophy blow-up in the limit of zero viscosity.

This is a much more complete physical description of isotropic turbulence than that obtained from the commonly used ϵ-transport model without vortex stetching which, for all initial conditions, predicts a power law decay where $k \sim t^{-1/(C_{\epsilon_2}-1)}$.

As far as anisotropic homogeneous turbulent flows are concerned, (36) can be generalized to the form

$$\dot{\epsilon} = \mathcal{P}_{\epsilon_S} + \frac{7}{3\sqrt{15}} \frac{C_{\epsilon_3}}{\sqrt{\nu}} \epsilon^{\frac{3}{2}} - C_{\epsilon_2} \frac{\epsilon^2}{k}, \tag{39}$$

where $\mathcal{P}_{\epsilon_S}$ is the production of dissipation by mean strains given by (8). In order to achieve closure, a model for $\mathcal{P}_{\epsilon_S}$ is needed. For simple homogeneously strained turbulent flows, it can be assumed that

$$\mathcal{P}_{\epsilon_S} \propto \mathcal{P} \tag{40}$$

which, after invoking elementary dimensional analysis, yields the model

$$\dot{\epsilon} = C_{\epsilon_1} \frac{\epsilon}{k} \mathcal{P} + \frac{7}{3\sqrt{15}} \frac{C_{\epsilon_3}}{\sqrt{\nu}} \epsilon^{3/2} - C_{\epsilon_2} \frac{\epsilon^2}{k}, \tag{41}$$

where C_{ϵ_1} is a dimensionless constant. The model for $\mathcal{P}_{\epsilon_S}$ in (40) has been used in the $k-\epsilon$ model of turbulence as well as in more complex second-order closures. Its success is largely tied to the fact that it constitutes a good approximation for plane shear flows (see Rogers et al., 1986 and Speziale and MacGiolla Mhuiris, 1989) – the type of flow being considered in this study. For practical calculations, C_{ϵ_1} can be taken to be 1.45 (a value obtained from equilibrium shear flows). In the next section, we will apply this model to homogeneous shear flow with $C_{\epsilon_1} = 1.45$, $C_{\epsilon_2} = 1.90$ and $C_{\epsilon_3} = 0.01$.

4 Illustrative Calculations for Homogeneous Shear Flow

In order to illustrate the effect of vortex stretching on homogeneous shear flow, we will present the results of calculations with a $k-\epsilon$ model for which the Reynolds stress tensor is modeled by

$$\tau_{ij} = \frac{2}{3} k \,\delta_{ij} - C_\mu \frac{k^2}{\epsilon} \left(\frac{\partial \bar{v}_i}{\partial x_j} + \frac{\partial \bar{v}_j}{\partial x_i} \right), \tag{42}$$

where $C_\mu = 0.09$ is a dimensionless constant. While the $k-\epsilon$ model is somewhat simplistic since it is based on an eddy viscosity, it was recently shown by Speziale and MacGiolla Mhuiris (1989) that this model is topologically equivalent to the more complex second-order closure models for homogeneous shear flow (the deficiencies in the $k-\epsilon$ model only become pronounced when there are combinations of shear and rotation or multi-dimensional strains). Hence, (42) will suffice to illustrate the qualitative changes induced when the effect of vortex stretching on the dissipation rate is accounted for. Equation (42) will be solved in conjunction with Eqs. (6) and (41). The standard $k-\epsilon$ model is recovered in the limit as $C_{\epsilon_3} \to 0$.

For homogeneous shear flow, the $k-\epsilon$ model with vortex stretching yields the transport equations

$$\dot{k} = C_\mu \frac{k^2}{\epsilon} S^2 - \epsilon \tag{43}$$

and

$$\dot{\epsilon} = C_{\epsilon_1} C_\mu k S^2 + \frac{7}{3\sqrt{15}} \frac{C_{\epsilon_3}}{\sqrt{\nu}} \epsilon^{\frac{3}{2}} - C_{\epsilon_2} \frac{\epsilon^2}{k} \tag{44}$$

which are obtained by substituting (4) into (6), (41) and (42).

For all nonzero values of C_{ϵ_3} it is a simple matter to show that the solution to (43) and (44) converges to an equilibrium state, with bounded energies. The equilibrium values may be found by setting the right-hand sides of (43)-(44) to zero, yielding the results

$$\frac{k_\infty}{k_0} = \frac{135}{49} \frac{\sqrt{C_\mu}(C_{\epsilon_2} - C_{\epsilon_1})^2}{C_{\epsilon_3}^2 R_{t_0}} \frac{Sk_0}{\epsilon_0} \tag{45}$$

and

$$\frac{\epsilon_\infty}{\epsilon_0} = \frac{135}{49} \frac{C\mu(C_{\epsilon_2} - C_{\epsilon_1})^2}{C_{\epsilon_3}^2 R_{t_0}} \left(\frac{Sk_0}{\epsilon_0} \right)^2. \tag{46}$$

These relations clearly indicate that k_∞/k_0 and $\epsilon_\infty/\epsilon_0$ have a $C_{\epsilon_3}^{-2}$ dependence so that the standard $k-\epsilon$ model prediction of an unbounded growth of k and ϵ is easily recovered in the limit as $C_{\epsilon_3} \to 0$.

Using (45) and (46) the following additional equilibrium values are also obtained for this $k-\epsilon$ model with vortex stretching:

$$\left(\frac{Sk}{\epsilon} \right)_\infty = \frac{1}{\sqrt{C_\mu}}, \tag{47}$$

$$\left(\frac{-\overline{uv}}{k} \right)_\infty = \sqrt{C_\mu} \tag{48}$$

and

$$R_{t_\infty} = \frac{135}{49} \frac{(C_{\epsilon_2} - C_{\epsilon_1})^2}{C_{\epsilon_3}^2}. \tag{49}$$

These results differ from the values of $(Sk/\epsilon)_\infty = \sqrt{\alpha/C_\mu}$, $(-\overline{uv}/k)_\infty = \sqrt{\alpha C_\mu}$, and $R_{t_\infty} = \infty$ obtained from the standard $k-\epsilon$ model where $\alpha \equiv (C_{\epsilon_2} - 1)/(C_{\epsilon_1} - 1) \approx 2$. Consistent with the conventional view of homogeneous shear flow, Sk/ϵ and $-\overline{uv}/k$ achieve equilibrium values that are independent of the initial conditions. The mechanism by which the presence of the vortex stretching term has the effect of creating bounded long time solutions lies in its enhancement of the growth rate of ϵ. Evidently, this increase in the growth rate of ϵ is accompanied by a simultaneous reduction in the production of k, thus forcing a production-equals-dissipation equilibrium. In alternative terms, vortex stretching—which becomes more pronounced at high turbulence Reynolds numbers since it scales as $\sqrt{R_t}$—eventually causes homogeneous shear flow to undergo a saturation to an equilibrium state with bounded component energies (the values of which are set by the shear rate, the viscosity and the initial conditions).

We will now show that the $k-\epsilon$ model with vortex stretching yields temporal evolutions of the turbulence fields for $St < 30$ that are in good qualitative agreement with previously conducted physical and numerical experiments. When nondimensionalized, (43)-(44) take the form

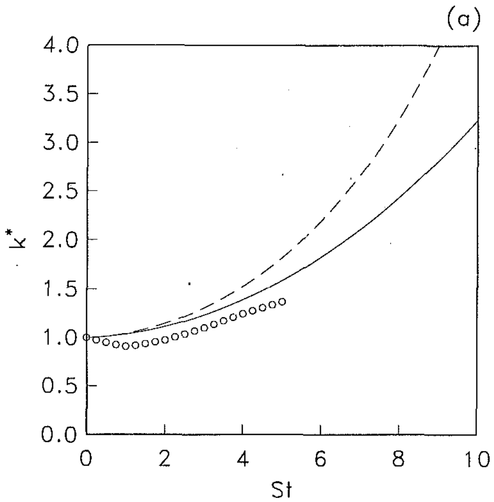

Fig. 7(a)

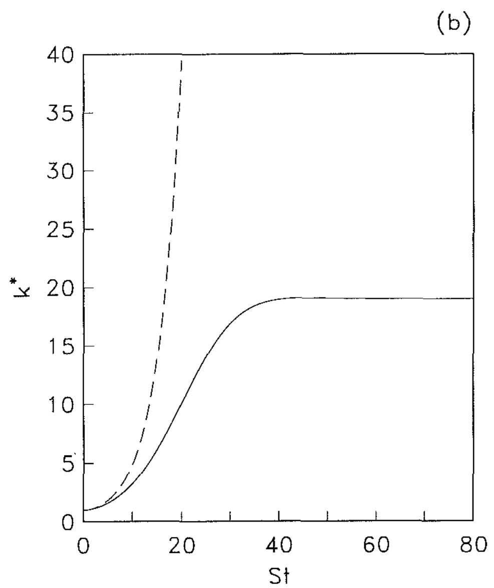

Fig. 7(b)

Fig. 7 Comparison of the model predictions with the large-eddy simulations of Bardina, et al. (1983) for homogeneous shear flow: o k^* from large eddy simulation; ——— k^* obtained from $k-\epsilon$ model with vortex stretching; --- k^* obtained from the standard $k-\epsilon$ model. (*a*) Short time solution, and (*b*) long time solution.

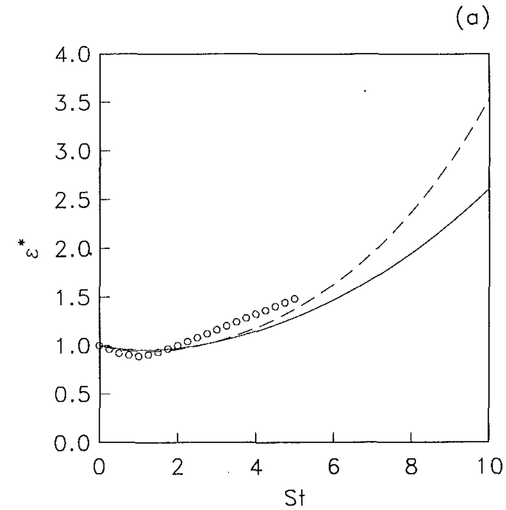

Fig. 8(a)

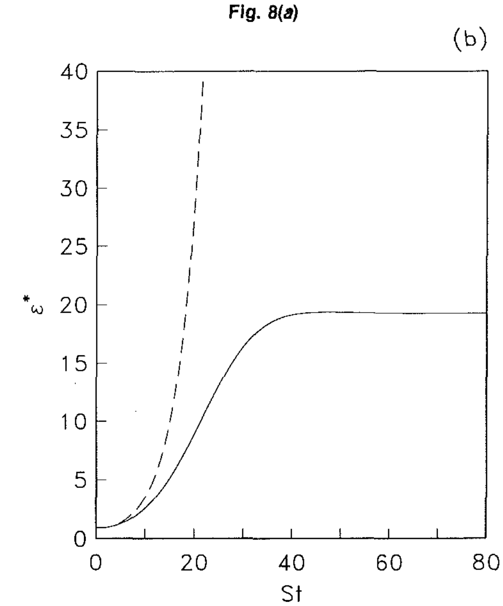

Fig. 8(b)

Fig. 8 Comparison of the model predictions with the large-eddy simulations of Bardina, et al. (1983) for homogeneous shear flow: o ϵ^* from large eddy simulation; ——— ϵ^* obtained from $k-\epsilon$ model with vortex stretching; --- ϵ^* obtained from the standard $k-\epsilon$ model. (*a*) Short time solution, and (*b*) long time solution.

$$\dot{k}^* = C_\mu \frac{Sk_o}{\epsilon_0}\frac{k^{*2}}{\epsilon^*} - \frac{\epsilon_0}{Sk_0}\epsilon^* \tag{50}$$

$$\dot{\epsilon}^* = C_{\epsilon_1}C_\mu \frac{Sk_0}{\epsilon_0}k^* + \frac{7}{3\sqrt{15}} C_{\epsilon_3}\frac{\epsilon_0}{Sk_0}\sqrt{R_{t_0}}\,\epsilon^{*\frac{3}{2}} - C_{\epsilon_2}\frac{\epsilon_0}{Sk_0}\frac{\epsilon^{*2}}{k^*} \tag{51}$$

where again we have $C_\mu = 0.09$, $C_{\epsilon_1} = 1.45$, $C_{\epsilon_2} = 1.90$ and $C_{\epsilon_3} = 0.01$ (the standard $k-\epsilon$ model is obtained by setting $C_{\epsilon_3} = 0$). The initial conditions, which correspond to an isotropic turbulence, are taken to be $\epsilon_0/Sk_0 = 0.296$ and $R_{t_0} = 300$. These are the approximate initial conditions of the large-eddy simulations of Bardina et al. (1983) which will allow us to make some direct comparisons between the model and the simulations.

Figures 7(*a*) and 8(*a*) display the short time solutions for k^* and ϵ^* compared to the large eddy simulation data. The solutions with vortex stretching are seen to display short term exponential growth in a manner very similar to that in the standard $k-\epsilon$ closure. The effect of the vortex stretching term is to reduce the growth rate of k^* and ϵ^*, though initially there is a slight increase in the magnitude of ϵ^*. A view of these solutions over a much longer time interval, as displayed in Figs. 7(*b*) and 8(*b*), reveals the dramatic effect that the vortex stretching term ultimately has on the long term growth of k^* and ϵ^*. It is seen that with the vortex stretching effect included, the initial exponential growth rates are eventually suppressed, so that by $St \approx 40$, k^* and ϵ^* asymptote to bounded equilibrium values.

Figures 9 and 10 show the short and long time behavior of the dimensionless ratios Sk/ϵ and $-\overline{uv}/k$ for the solutions obtained both with and without vortex stretching. The curves in Figs. 9(*a*) and 10(*a*) give the impression that an equilibrium state for these quantities may have been achieved by the time $St \approx 10$. However, the long time solutions in Figs. 9(*b*) and 10(*b*) reveal that, in the case where vortex stretching effects are included, only a local maximum is reached – further developments must occur before a true equilibrium is achieved.

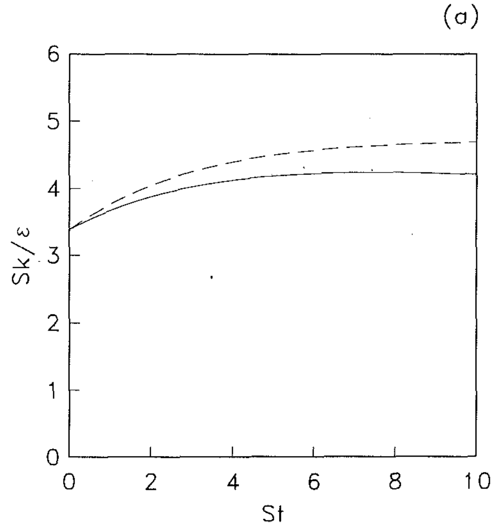

Fig. 9(*a*)

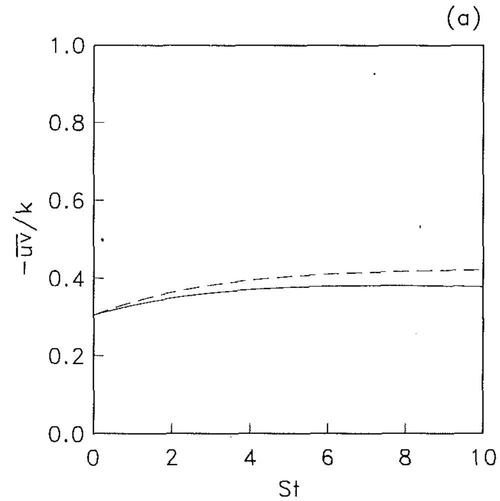

Fig. 10(*a*)

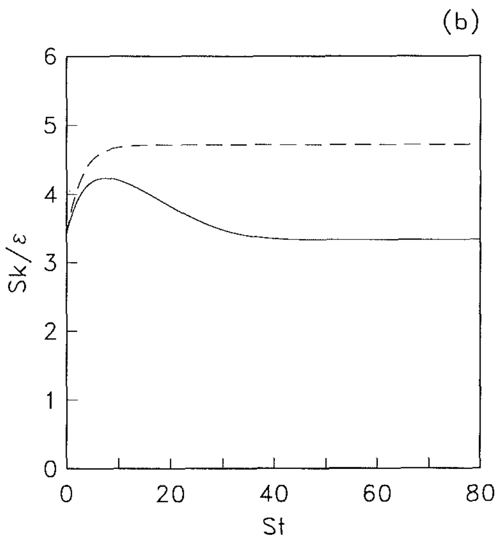

Fig. 9(*b*)

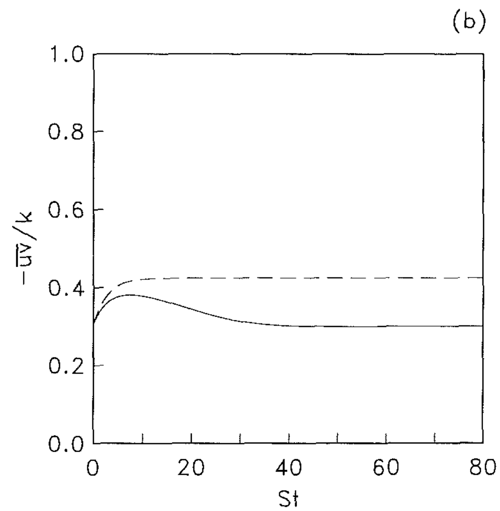

Fig. 10(*b*)

Fig. 9 Comparison of the model predictions for Sk/ϵ: ——— $k-\epsilon$ model with vortex stretching; --- standard $k-\epsilon$ model. (*a*) Short time solution, and (*b*) long time solution.

Fig. 10 Comparison of the model predictions for $-\overline{uv}/k$: ——— $k-\epsilon$ model with vortex stretching; --- standard $k-\epsilon$ model. (*a*) Short time solution, and (*b*) long time solution.

This suggests that the apparent convergence of quantities such as Sk/ϵ seen in numerical and experimental studies, may not signify that a final equilibrium state has resulted (i.e., it may only be a local maximum). The behavior of Sk/ϵ shown in Fig. 9(*b*) with vortex stretching present is remarkably consistent from a qualitative standpoint with the direct simulations of Rogers et al. (1986) shown in Fig. 11 (i.e., the tails in Sk/ϵ as time increases in the computations of Rogers et al., 1986 could indicate that an equilibrium state has not been reached).

Figure 12 provides a plot of the long time behavior of the computed turbulence Reynolds number. It achieves an equilibrium value of approximately 5600, which is more than eighteen times its initial value. The most significant effect of the vortex stretching term on k^* and ϵ^*, as seen in Figs. 7(*b*) and 8(*b*), occurs for $R_t > 4000$. This confirms the belief that vortex stretching is mostly a phenomenon associated with high turbulence Reynolds numbers. Some indication of the sensitivity of the computed solutions to the imbalance in the vortex stretching as characterized by C_{ϵ_3} is shown in Fig. 13. This contains the time evolution of k^* for a range of values of C_{ϵ_3}; as expected, k^*_∞ increases with decreasing values of C_{ϵ_3}. Figure 14 shows the effect on k^* of a change in the initial

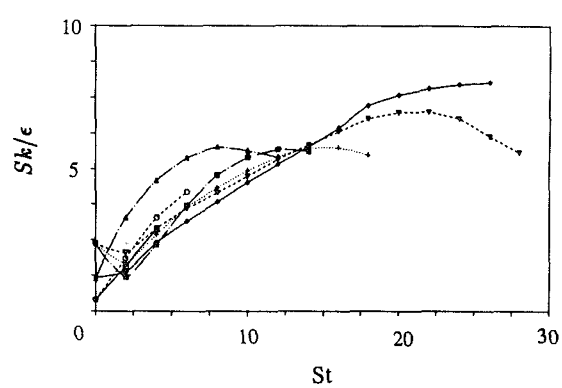

Fig. 11 Time evolution of Sk/ϵ taken from the direct numerical simulations of Rogers et al. (1986) on homogeneous shear flow.

values of ϵ/Sk. As would be expected on physical grounds, an increase in the dimensionless shear rate leads to a higher equilibrium value for the turbulent kinetic energy.

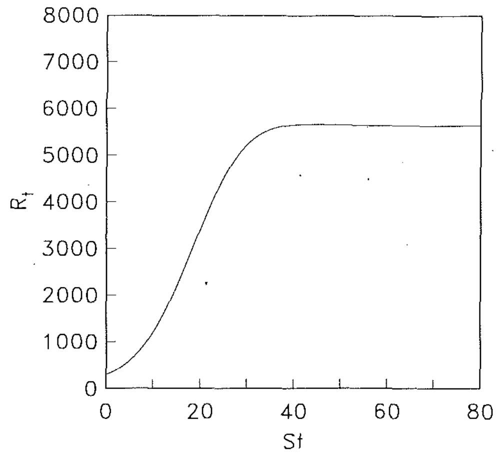

Fig. 12 Time evolution of the turbulence Reynolds number R_t predicted by the $k-\epsilon$ model with vortex stretching.

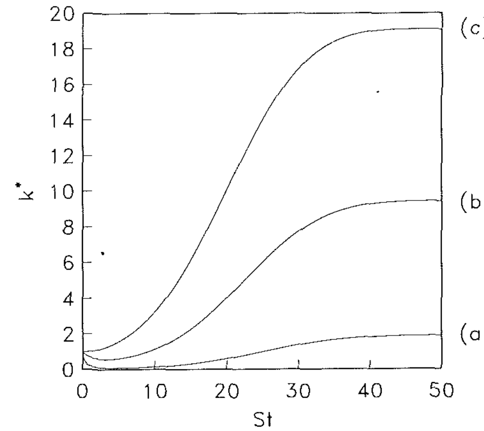

Fig. 14 Sensitivity of the model predictions for the turbulent kinetic energy to ϵ_0/Sk_0: (*a*) $\epsilon_0/Sk_0 = 3.0$; (*b*) $\epsilon_0/Sk_0 = 0.6$, and (*c*) $\epsilon_0/Sk_0 = 0.296$.

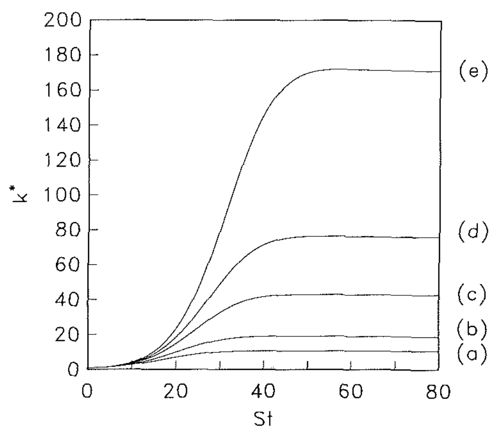

Fig. 13 Sensitivity of the model predictions for the turbulent kinetic energy to C_{ϵ_3}: (*a*) $C_{\epsilon_3} = 0.0133$, (*b*) $C_{\epsilon_3} = 0.01$; (*c*) $C_{\epsilon_3} = 0.0066$; (*d*) $C_{\epsilon_3} = 0.005$, and (*e*) $C_{\epsilon_3} = 0.0033$.

5 Conclusions

An alternative view concerning the equilibrium structure of homogeneous turbulent shear flow has been presented based on maintaining the effect of vortex stretching. It was shown that the presence of just a small net vortex stretching term in the dissipation rate equation can ultimately drive the flow to a production-equals-dissipation equilibrium with bounded energy states. For elapsed times $St < 30$—which includes the largest values of St considered in any of the previously conducted physical or numerical experiments—the introduction of this small unbalanced vortex stretching term into the standard modeled dissipation rate transport equation still yields an exponentially growing turbulent kinetic energy and dissipation. However, since this vortex stretching term scales as $\sqrt{R_t}$, it eventually becomes dominant, causing a saturation of the system to a production-equals-dissipation equilibrium with bounded turbulent kinetic energy and dissipation. Although this alternative physical picture of homogeneous shear flow is contrary to the commonly accepted asymptotic laws—for which an unbounded exponential time growth of k and ϵ is postulated—it is a real possibility that should be seriously considered in the future. The plausibility of these results were supported by independent calculations of isotropic turbulence which demonstrated that the inclusion of this vortex stretching effect yields a much more complete physical description. In fact, the calculations suggested that a $k \sim t^{-1}$ power law decay is the equilibrium state toward which a high-Reynolds-number isotropic turbulence is driven in order to resolve the $O(R_t^{1/2})$ imbalance between vortex stretching and viscous diffusion. As alluded to earlier, the results obtained in this study—for isotropic decay as well as for homogeneous shear flow—are qualitatively the same as those obtained from the theory of self-preservation (see Speziale and Bernard, 1991).

New physical and numerical experiments on homogeneous shear flow, for larger elapsed times St, could shed more light on the issue. The recent experiments of Tavoularis and Karnik (1989), which were conducted up to $St = 28$, did show some tendency of the integral length scales to level off—a feature which, if more solidly established, would be supportive of the existence of a production-equals-dissipation equilibrium. However, even if the integral length scales do grow without bound—and this is a distinct possibility since the flow field is infinite—it is still possible for the kinetic energy and dissipation rate to equilibrate to bounded values (it should be remembered that the integral length scales grow without bound in isotropic decay).

Finally, some comments should be made concerning the implications of the results of this paper for turbulence modeling. Since all of the commonly used two-equation models and second-order closures based on the turbulent dissipation rate equation neglect this vortex stretching effect, they predict an unbounded exponential time growth of k and ϵ in homogeneous shear flow. This type of behavior has been shown to cause problems in the calculation of certain inhomogeneous turbulent flows. The singularity in plane stagnation point turbulent flow represents a prime example (Speziale, 1989). Hence, the alteration of turbulence models to yield a production-equals-dissipation equilibrium in homogeneous shear flow via vortex stretching could make their behavior more robust in other turbulent flows without compromising their ability to predict results consistent with physical and numerical experiments on homogeneous turbulence. Whether or not homogeneous shear flow actually saturates to a production-equals-dissipation equilibrium remains an open question that will probably only be resolved by a rigorous mathematical proof based on an appropriate energy norm. For the meantime, however, the results of this study appear to establish the need to re-examine this issue.

Acknowledgments

The authors are indebted to Dr. M. M. Rogers (NASA Ames) for his helpful comments and for allowing us to use unpublished results from his direct simulations on homogeneous shear flow. Funding provided to P. S. Bernard through an ASEE/Navy Summer Faculty Research Fellowship at the Naval Research Laboratory, Washington, DC is greatly appreciated.

C.G. Speziale acknowledges the support of the National Aeronautics and Space Administration under NASA Contract No. NAS1-18605 while in residence at ICASE.

References

Bardina, J., Ferziger, J. H., and Reynolds, W. C., 1983, "Improved Turbulence Models Based on Large-Eddy Simulation of Homogeneous, Incompressible Turbulent Flows," *Stanford Univ. Report TF - 19.*

Batchelor, G. K., and Townsend, A. A., 1947, "Decay of Isotropic Turbulence in Initial Period," *Proc. R. Soc. London*, Series A, Vol. 193, pp. 539–558.

Bernard, P. S. 1985, "Energy and Vorticity Dynamics in Decaying Isotropic Turbulence," *Int'l J. Engrg. Sci.*, Vol. 23, pp. 1037–1057.

Champagne, F. H., Harris, V. G. and Corrsin, S., 1970, "Experiments on Nearly Homogeneous Turbulent Shear Flow," *J. Fluid Mech.*, Vol. 41, pp. 81–139.

Comte-Bellot, G., and Corrsin, S., 1971, "Simple Eulerian Time Correlation of Full- and Narrow-Band Velocity Signals in Grid-Generated, Isotropic Turbulence," *J. Fluid Mech.*, Vol. 48, pp. 273–337.

Corrsin, S., 1963, *Handbuch der Physik VIII/2*, ed. S. Flugge and C. Truesdell, Springer, New York, p. 524.

Harris, V. G., Graham, J. A., and Corrsin, S., 1977, "Further Experiments in Nearly Homogeneous Turbulent Shear Flow," *J. Fluid Mech.*, Vol. 81, pp. 657–687.

Hinze, J. O., 1975, *Turbulence*, (McGraw-Hill, NY)

Lesieur, M., 1990, *Turbulence in Fluids*, 2nd Edition, (Martinus Nijhoff, Boston).

Pumir, A., and Siggia, E., 1990, "Collapsing Solutions to the 3D Euler Equations," *Phys. Fluids A*, Vol. 2, pp. 220–241.

Rogallo, R. S., 1981, "Numerical Experiments in Homogeneous Turbulence," NASA Technical Memorandum 81315.

Rogers, M. M., 1990, *Private Communication.*

Rogers, M. M., Moin, P. and Reynolds, W. C., 1986, "The Structure and Modeling of the Hydrodynamic and Passive Scalar Fields in Homogeneous Turbulent Shear Flow," *Stanford Univ. Report TF - 25.*

Rohr, J. J., Itsweire, E. C., Helland, K. N. and Van Atta, C. W., 1988, "An Investigation of the Growth of Turbulence in a Uniform Mean Shear Flow," *J. Fluid Mech.*, Vol. 187, pp. 1–33.

Rose, W. G., 1966, "Results of an Attempt to Generate a Homogeneous Turbulent Shear Flow," *J. Fluid Mech.*, Vol. 25, pp. 97–120.

Sedov, L. I., 1944, "Decay of Isotropic Turbulent Motions of an Incompressible Fluid," *Doklady Akademie Nauk, SSSR*, Vol. 42, pp. 116–119.

Speziale, C. G., 1989, "On the Free Stream Matching Condition for Stagnation Point Turbulent Flows," *Forum on Turbulent Flows*, ed. W. W. Bower and M. J. Morris, ASME, New York, FED - Vol. 76, pp. 19–24.

Speziale, C. G., and Bernard, P. S. 1991, "The Energy Decay in Self-Preserving Isotropic Turbulence Revisited," *ICASE Report No. 91-58*, NASA Langley Research Center. (To appear in J. Fluid Mech.).

Speziale, C. G., and MacGiolla Mhuiris, N., 1989, "On the Prediction of Equilibrium States in Homogeneous Turbulence," *J. Fluid Mech.*, Vol. 209, pp. 591–615.

Tavoularis, S., 1985, "Asymptotic Laws for Transversely Homogeneous Turbulent Shear Flows," *Phys. Fluids*, Vol. 28, pp. 999–1004.

Tavoularis, S., and Corrsin, S., 1981, "Experiments in Nearly Homogeneous Turbulent Shear Flows With a Uniform Mean Temperature Gradient, Part 1," *J. Fluid Mech.*, Vol. 104, pp. 311–347.

Tavoularis, S., and Karnik, U., 1989, "Further Experiments on the Evolution of Turbulent Stresses and Scales in Uniformly Sheared Turbulence," *J. Fluid Mech.*, Vol. 204, pp. 457–478.

Tennekes, H., and Lumley, J. L, 1972, *A First Course in Turbulence*, M.I.T. Press, Cambridge, MA.

Townsend, A. A., 1956, *The Structure of Turbulent Shear Flow*, Cambridge University Press, New York.

Von Karman, T., 1937, "The Fundamentals of the Statistical Theory of Turbulence," *J. Aero Sci.*, Vol. 4, pp. 131–138.